Study of direct photon production in Pb-Pb collisions at $\sqrt{s_{NN}} = 5.02$ TeV with ALICE experiment's Photon Spectrometer(PHOS) at Large Hadron Collider

Sushobhan Kumar Mandal

National Center for Nuclear Research

Warsaw, Poland

May 9, 2024

Overview

Standard model and strong interaction

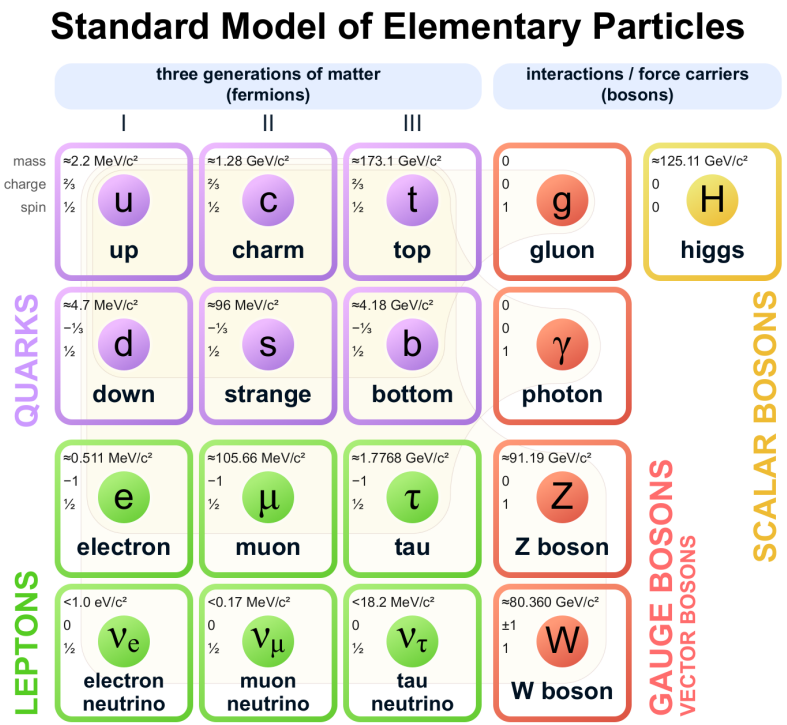

Figure: Standard model of particle physics [1]

- Quarks and leptons participate in weak interaction
- Electrically charged leptons and quarks participate in EM interaction
- Quarks and Gluons carry three types of color charges
- Gluons act as mediators between the quarks resulting strong interaction
- Bound states of quarks are formed resulting ordinary matter(baryons, mesons and others) around us

Strength Comparison The strength (in dimensionless coupling const.) of the weak interaction is $\sim 10^{-6}$ [range: 10^{-18}m] , the electromagnetic interaction is $\sim$1/137 [range: ∞], and strong interaction is $\sim$1 [range: 10^{-15}m]

[1] Image source: [wikipedia]

Features of Quantum Chromodynamics(QCD)

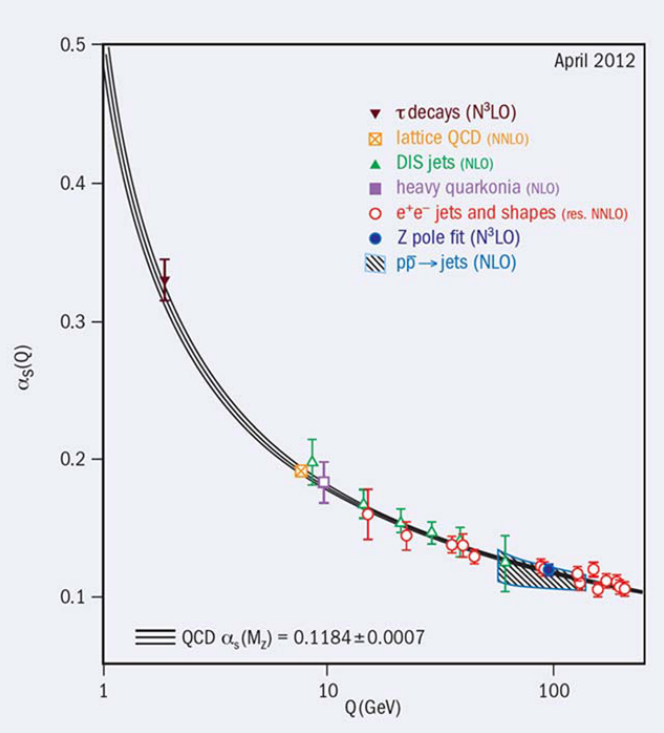

Figure: $\alpha_s(Q^2) = \frac{4\pi}{\beta_0 \times ln(Q^2/\Lambda^2)}$, the effective coupling strength decreases as a function of increasing interaction energy(Q) or decreasing distance [2]. (Gross, Wilczek and Politzer received Nobel Prize in 2004 for Asymptotic freedom in in QCD)

- Color confinement: Free colour charges do not exist int the nature. Attempt to separate them causes spontaneous creation of a quark–antiquark pair
- Chiral symmetry breaking: The process of spontaneous global symmetry breaking that explains the masses of hadrons way greater [∼99% of the proton's mass comes from QCD interaction] than the masses of quarks
- **Asymptotic freedom :** As the energy of the interaction increases, the strong interaction weakens, leading quarks and gluons to behave much like free particles. This enables us to apply perturbation theory in QCD.

[1] Figure 3 in Siegfried Bethke "World Summary of α_s (2012)" MPP-2012-132 arXiv:1210.0325 [hep-ex].

Phase transition in QCD and Quark-gluon plasma(QGP)

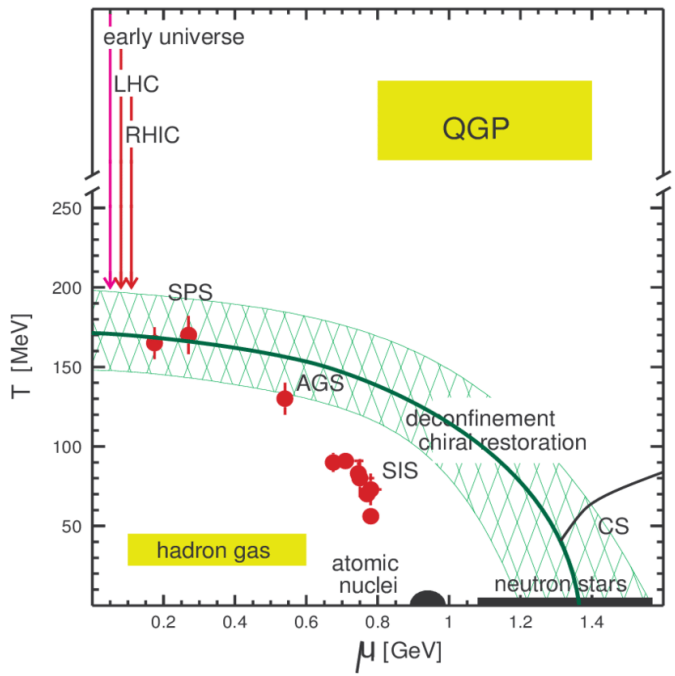

Figure: QCD Phase diagram : Several experiments have probed and still probing different regions of the phase diagram to understand the collective properties of quarks and gluons in various situations

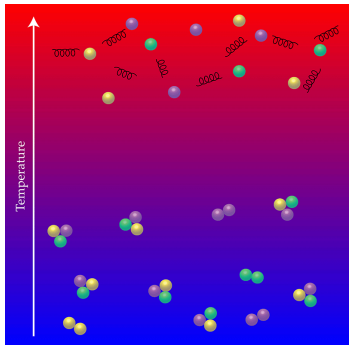

- If we increase the energy density[3] **($\sim$1 GeV/fm^3)** over a large volume by compressing (i.e., by increasing the chemical potential)
  or heating[4] **($\sim$170 MeV)** or combining both the processes, the hadronic matter is expected to enter a deconfined phase exhibiting fluid like properties

- Lattice gauge theory loses its applicability at finite μ_B. The phase diagram has to be explored by comparing experimental results with effective models

[3] Karsch, Lect. Notes Phys., 209 (2002), hep-lat/0106019; [4] Borsanyi et al., JHEP 1009 (2010) 073 [arXiv:1005.3508[hep-lat]]

Early universe and Quark deconfinement

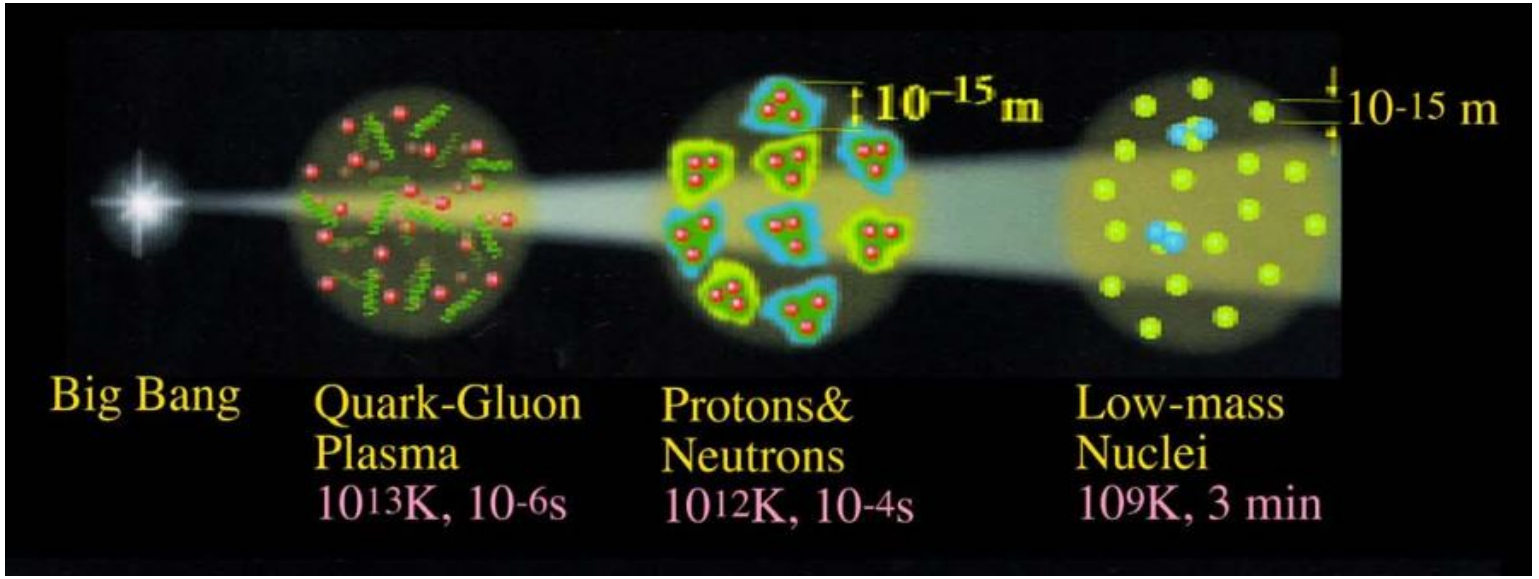

- After big bang (few microseconds old) universe is believed to be filled with deconfined state of quarks and gluons.
- Heavy-ion collisions recreate in the labs, such droplets of matter that filled the universe about $\sim 1 \mu S$ after the big bang
- With heavy-ion collisions we can learn about the properties (Not possible with astronimcal) at very temperature and density and explore QCD phase diagram

[4] picture: ncatlab.org;

Advantages of nucleus-nucleus(e.g. Au, Cu, Pb) collisions over p-p collisions in the study of QCD phase diagram and QGP

- Energy density:
  - p-p collisions: Typically a few GeV/fm^3
  - A-A collisions: 10-20 GeV/fm^3 or higher
- Temperature:
  - A-A collisions: Several hundred MeV to over a trillion degrees Kelvin
- Size and lifetime of the QGP:
  - p-p collisions: Highly transient and smaller in size
  - A-A collisions: Spatial extent of several femtometers, lasting tens to hundreds of femtoseconds
- Particle multiplicity:
  - A-A collisions: Significantly larger number of particles compared to p-p collisions

Evolution of the medium and QGP signatures

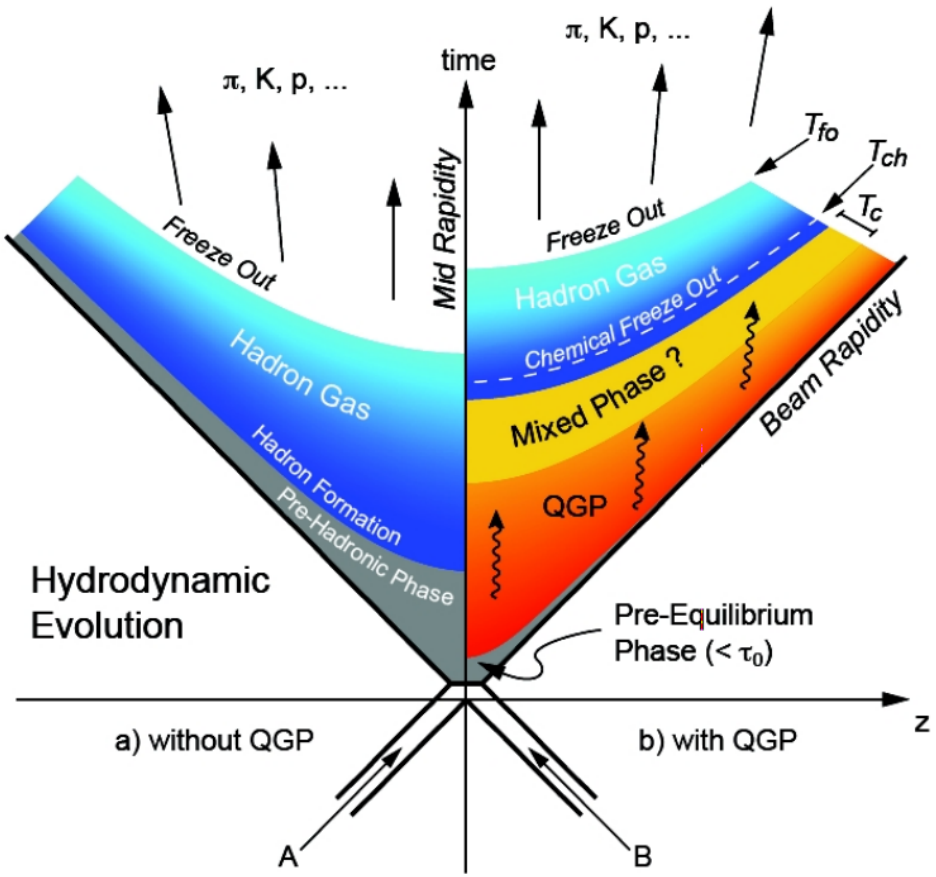

Figure: Evolution of QGP after high energy coliisions

Different ways of probing QGP

- Jet quneching (Energy modification of high-p_T jets)
- Di-lepton production ($q\bar{q} \rightarrow \mu\bar{\mu}$)
- Strangeness production ($q\bar{q} \rightarrow s\bar{s}$, $g\bar{g} \rightarrow s\bar{s}$)
- Charmonium suppression (J/ψ suppression)
- Direct photon production ($q\bar{q} \rightarrow g\gamma$, $qq \rightarrow qq\gamma$ etc.)

[4] https://particlesandfriends.wordpress.com/2016/10/14/evolution-ofcollisions-and-qgp/

My research topic: Direct photon study in heavy-ion collisions

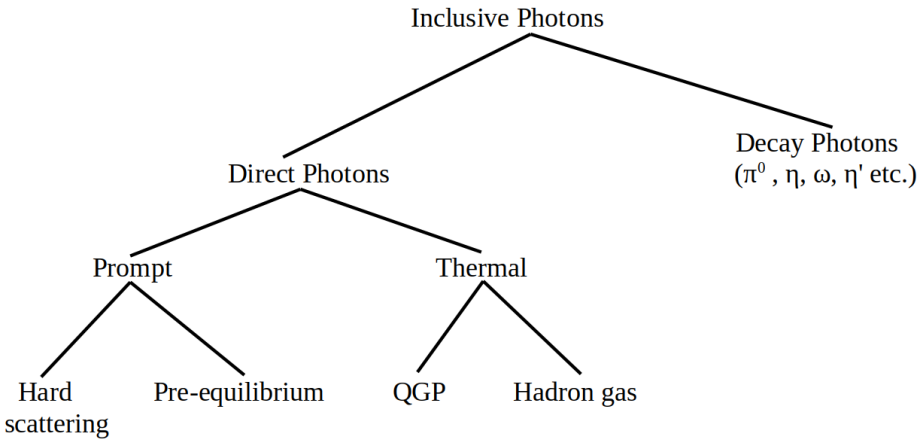

Figure: Photon production in high energy collisions

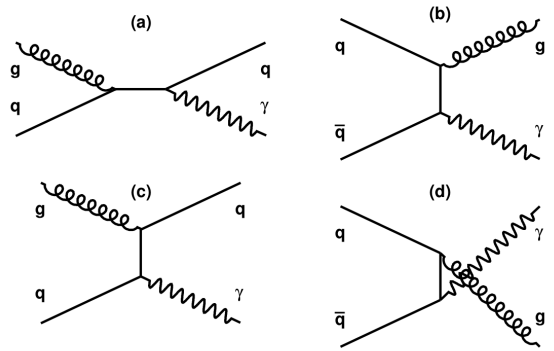

Figure: Direct photon production in Compton scattering (a and c) and pair annihilation (b and d) processes

- Direct photons refer to photons that are produced directly in the initial stages of the heavy-ion collision, through the interactions of the quarks and gluons belonging to initial colliding particles
- The photons are not affected by the strong interaction, and they provide a clean probe of the properties of the deconfined quark-gluon matter. By studying the production and properties of direct photons, we can learn about the temperature, pressure, and other properties of the QGP.

Large Hadron Collider and A Large Ion Collider Experiment(ALICE)

Figure: LHC aerial view

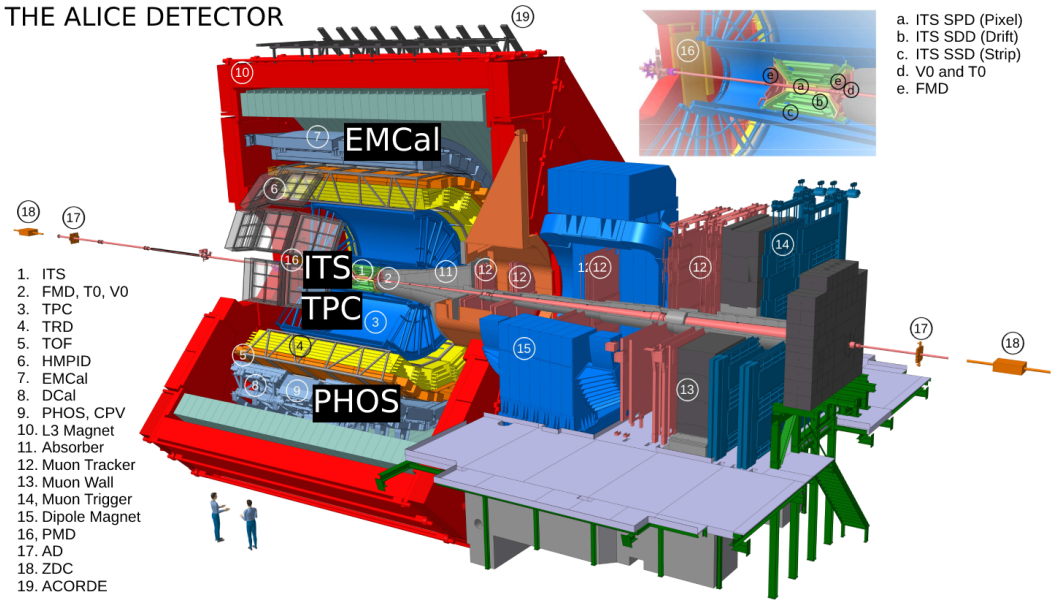

Figure: ALICE schematics during Run2

[4] cern.ch, alice-collaboration.web.cern.ch

Coordinate system in ALICE

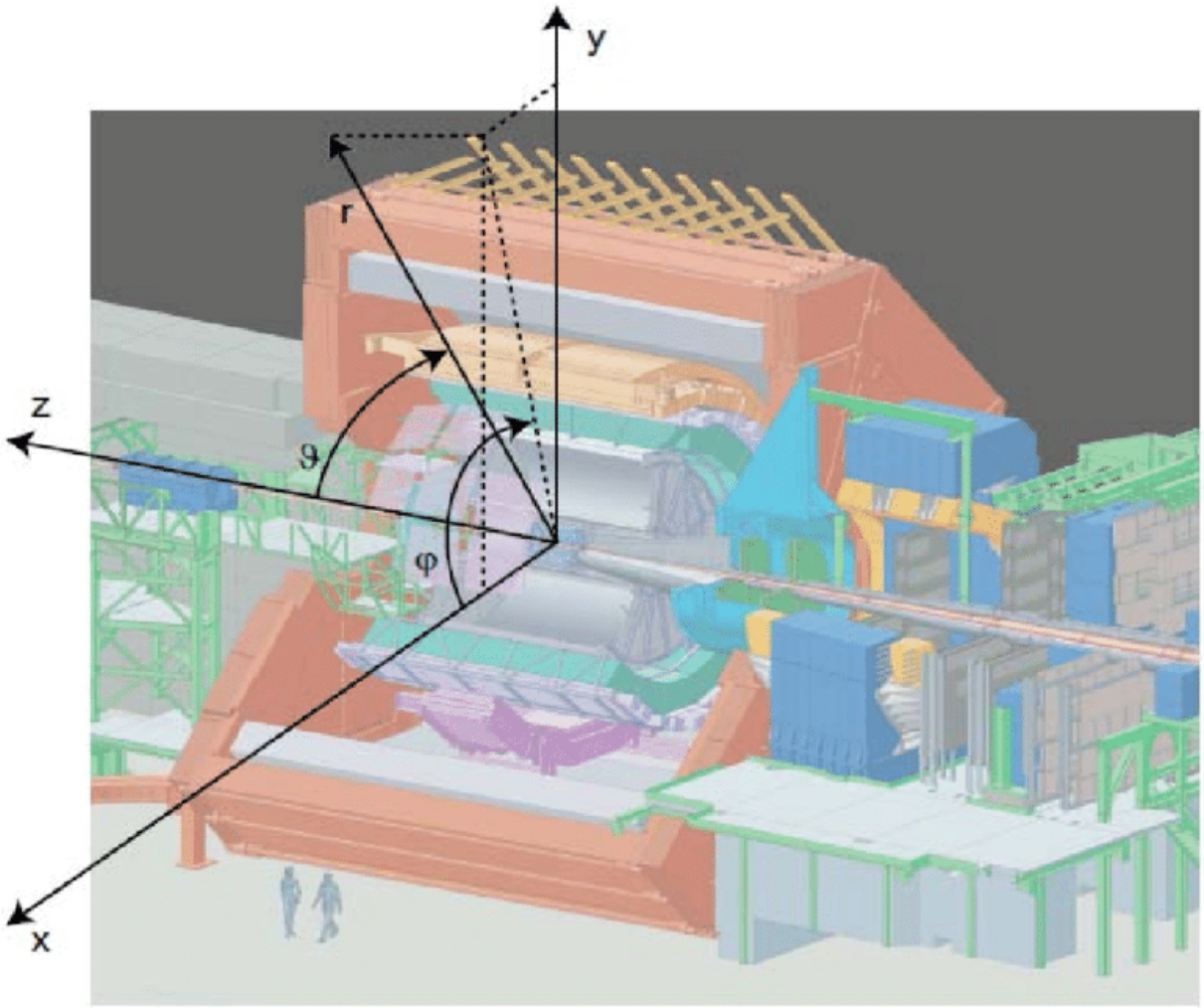

Figure: Like other major experiments at LHC, (θ, ϕ, z) co-ordinate system is used at ALICE . Pseudo-rapidity $\eta = -ln(tan\frac{\theta}{2})$

[4] https://doi.org/10.1016/j.cpc.2021.108206

PHOton Spectrometer(PHOS)

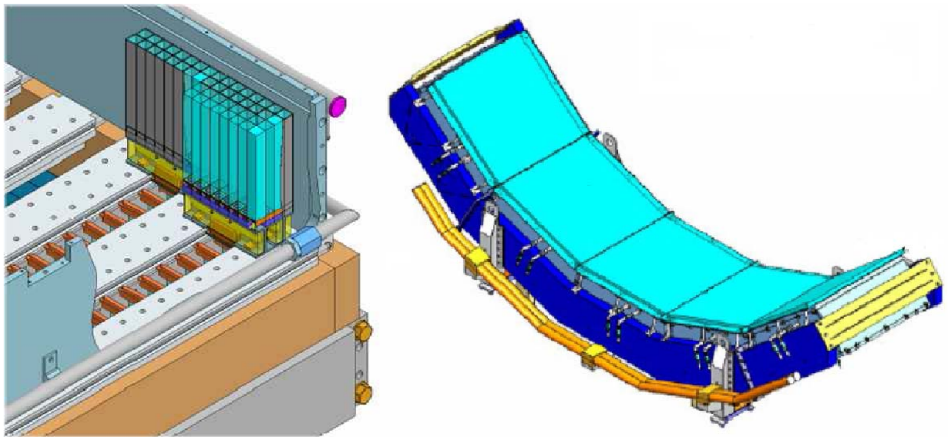

Figure: Photon detetction modules in the ALICE experiment

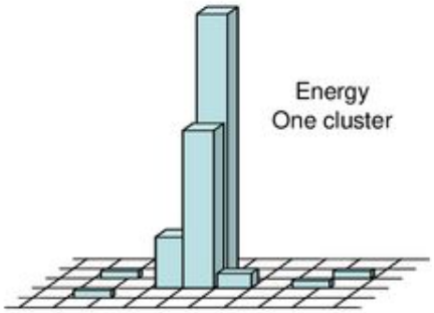

Figure: Cluster formed by energy deposition in the PHOS cells

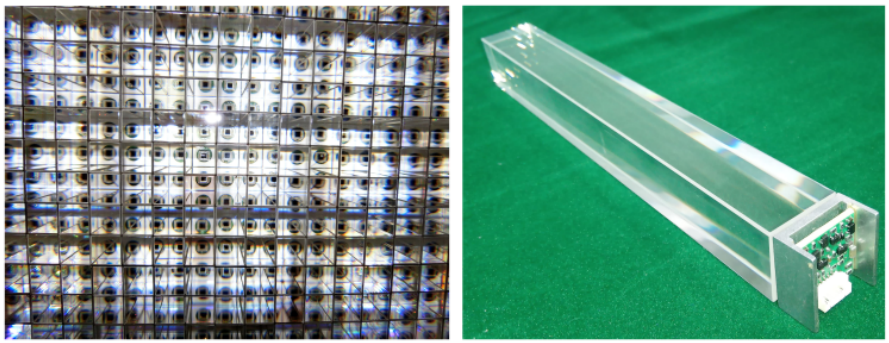

Figure: PHOS cell matrix[left]; A detector element consisting $PbWO_4$ crystal, APD(Avalanche Photo Diode) detector and preamplifier[right]

- Almost 80% of the total cluster energy is deposited in the central cell
- Good at measuring both low energy range and high energy range : 100 MeV to 100 GeV
- At energy range $>$1GeV, the precision is approx. given by $\frac{\sigma_E}{E} = \frac{3\%}{\sqrt{E}} \pm 0.8\%$

[4] alice-collaboration.web.cern.ch

Collision centrality : $\left(\frac{spectator}{All}\right)$

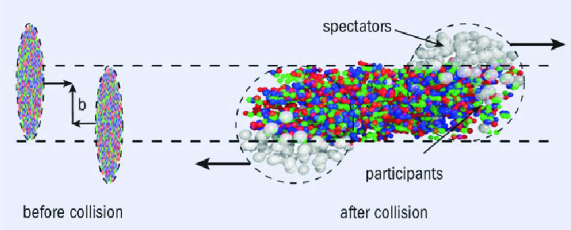

Figure: centrality is the ratio of spectator nucleons to the total no. of nucleons

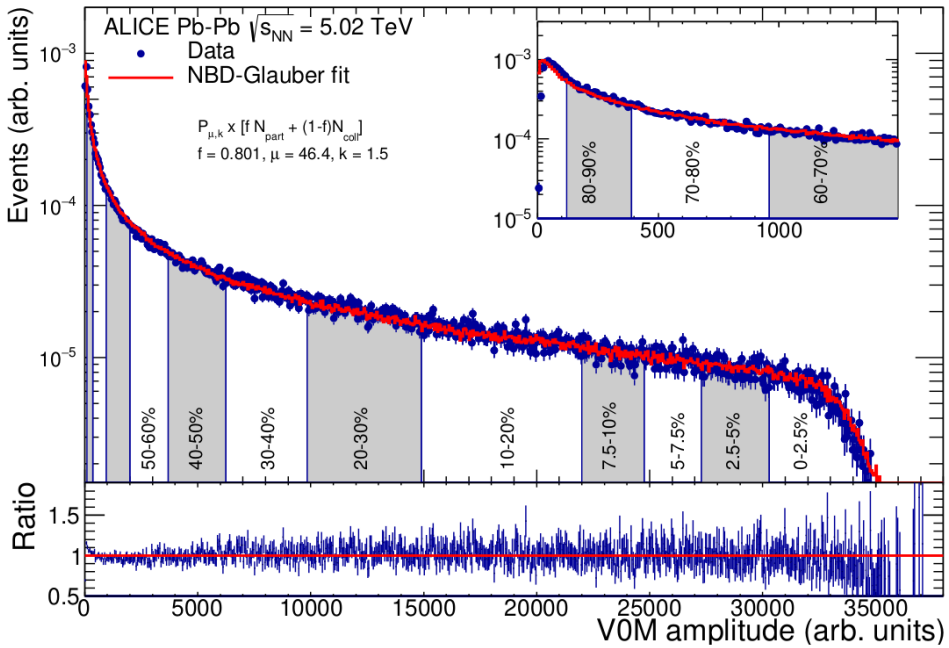

Figure: Distribution of the sum of amplitudes in the V0 scintillators for Pb–Pb collisions at $\sqrt{s_{NN}} = 5.02$ TeV. The distribution is fitted with the NBD-Glauber fit shown as a line. The inset shows a zoom of the most peripheral region.

[4] Centrality determination in heavy ion collisions, ALICE-PUBLIC-2018-011

Statistics of the data, events and clusters selection

Run period	Range of run numbers	Number of selected runs	Total statistics
LHC18r	296690-297624	58	41.234×10^6
LHC18q	295581-296623	131	64.970×10^6

Table: Statistics of the data used in our analysis

Event selection criterion

- To avoid pile-up of events we impose the following restrictions: Number of vertex=1;
- Z-coordinate of the vertex $\leq$10.0 cm.
- To exclude false signals, we choose the number of contributors (reconstructed charged particle tracks)$\geq$1.

Cluster selection criterion

- clusters satisfy PHOS neutrality condition
- minimum energy of E $\geq$ 0.3 GeV
- minimum number of cells Ncells $\geq$ 3
- time of flight of the photons TOF $\leq$ 12.5 ns
- size of the cluster $\geq$ 0.1 cm

Reconstructing the Invariant mass of π^0 meson from two photons decay

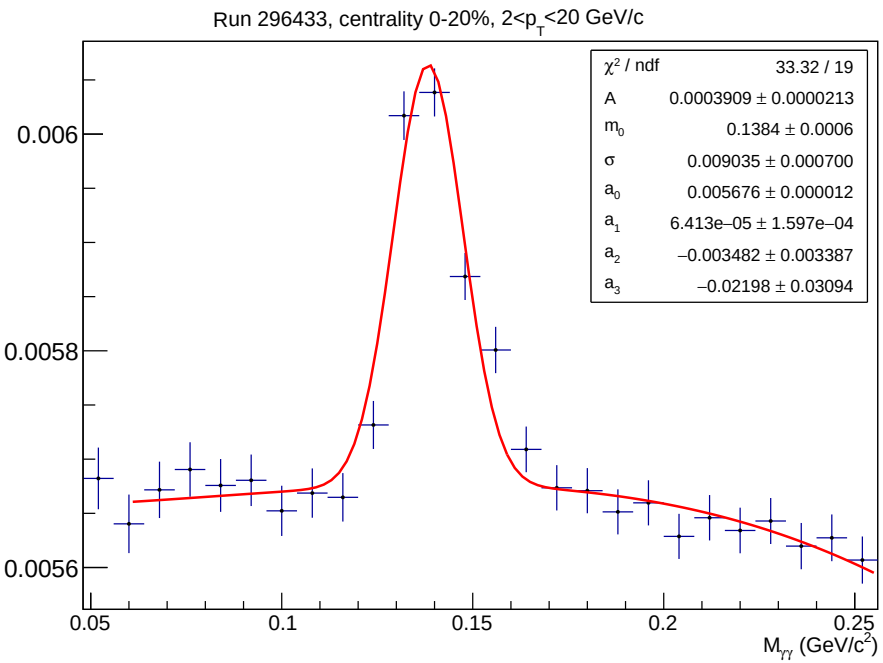

Figure: Invariant mass of π^0 in a particular run(296433) in a given centrality(00-20%) by fitting the signal with gaussian and the combinatorial background by 3rd order polynomial

- $\pi^0 \rightarrow \gamma + \gamma$ (BR : 98.8%)
- Invariant mass of two photons, $M_{\gamma\gamma} = \sqrt{2E_{\gamma_1}E_{\gamma_2}(1-\cos\theta)}$
- Signal (Gaussian) : $A \cdot \exp\left[-\frac{(m-m_0)^2}{2\sigma^2}\right]$
- Background (3rd order polynomial) : $a_0 + a_1(m-m_0) + a_2(m-m_0)^2 + a_3(m-m_0)^3$

Data quality assurance: Run-by-run study of π^0 peak position

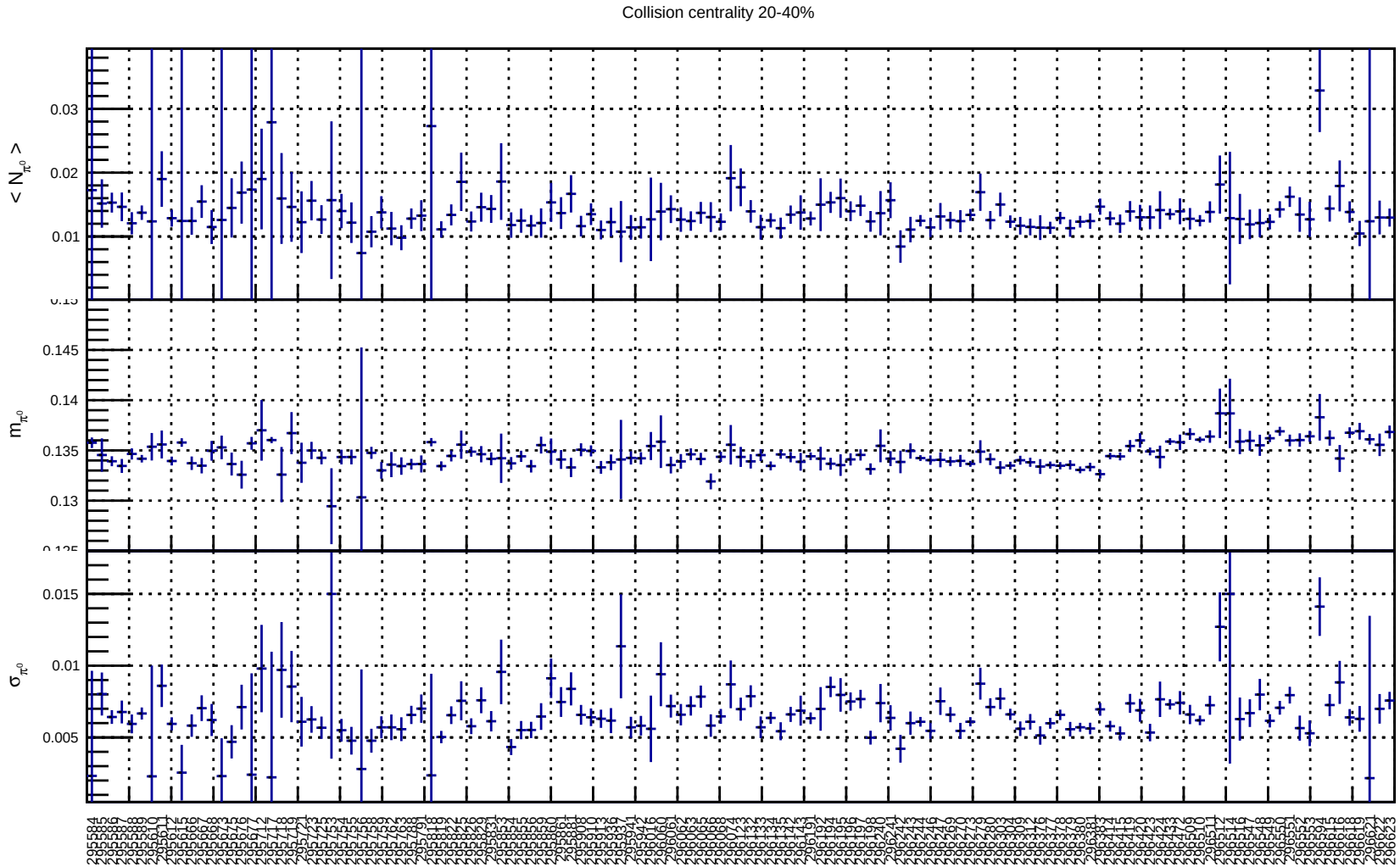

Figure: The run numbers corresponding to the run period LHC18q is given in the x-axis

E/p ratio of measurements for electrons(and positrons)

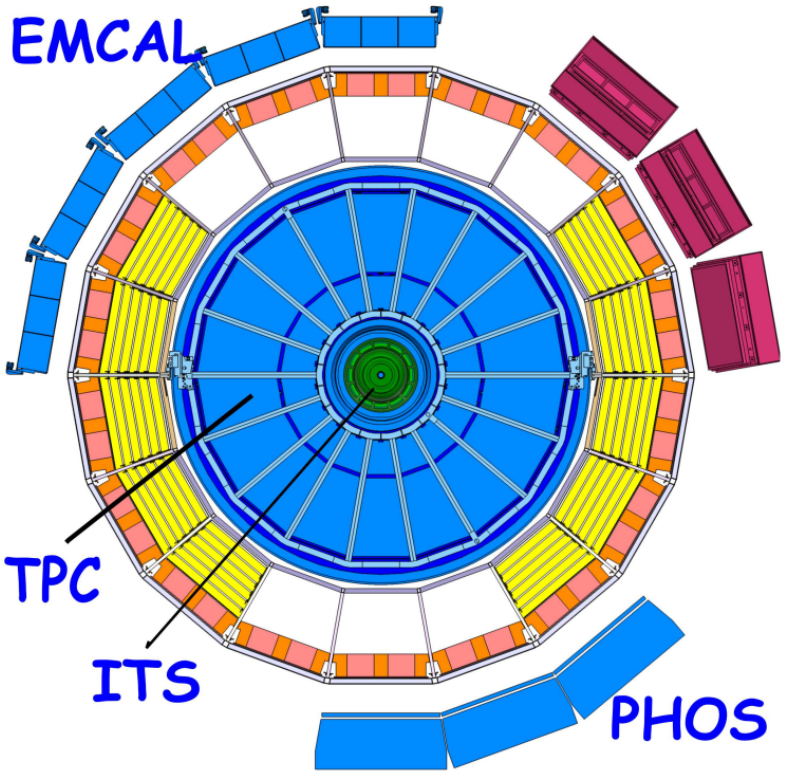

Figure: Independent measurements of momenta (in ITS and TPC) and energy (in PHOS) of electrons(and positrons)

- $E = \sqrt{(p^2 + m_e^2)}$
- $m_e = 0.0005 GeV << p(\sim GeV)$
- E ≈ p or, E/p ≈ 1
- 'p' is measured by ITS and TPC using curvature of the trajectory whereas 'E' is measured in PHOS

Calibration of PHOS: E/p ratio of beta particles in run period LHC18r

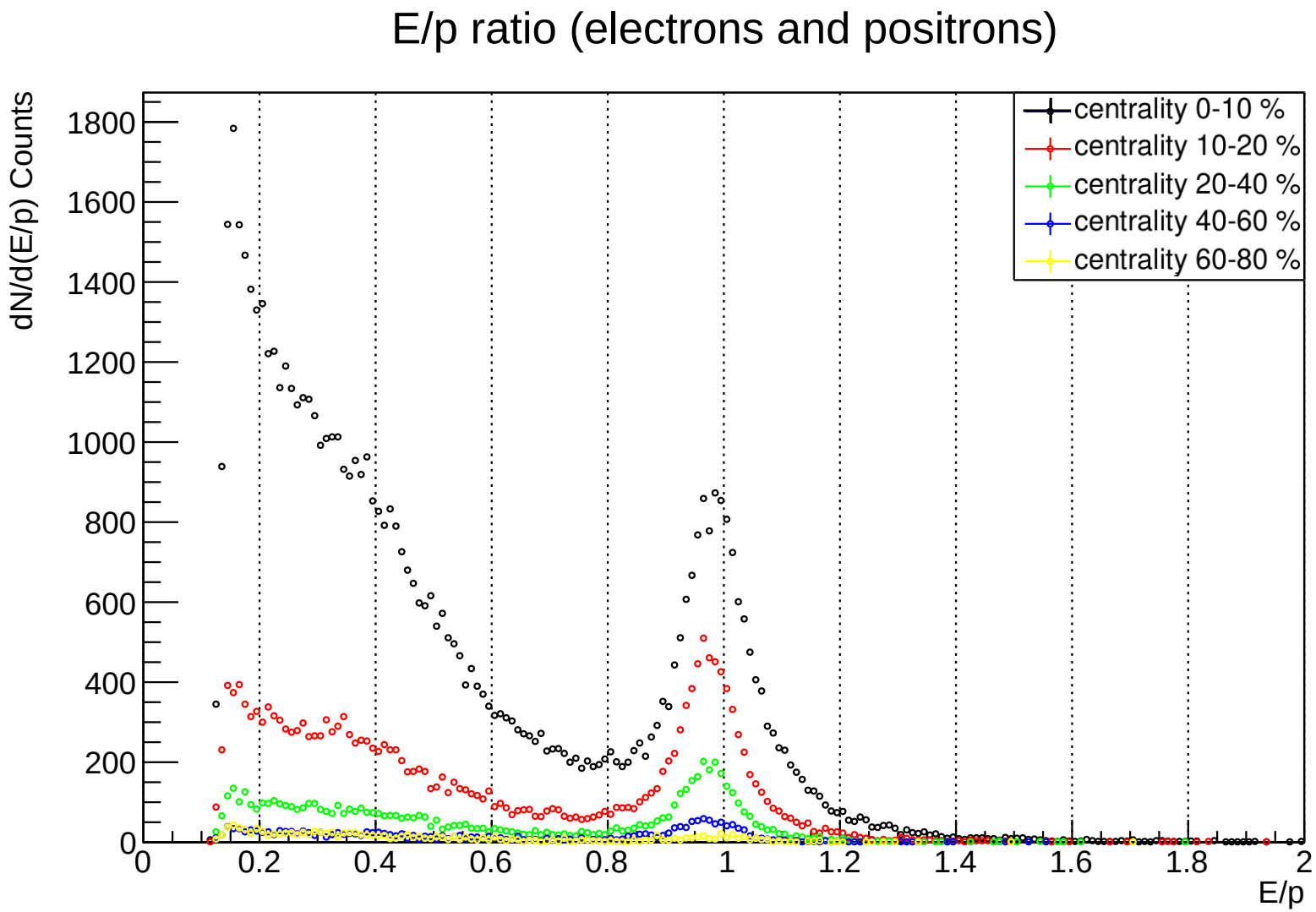

Figure: Differential count vs E/p ratio of electrons

Inclusive photons(γ^{inc}), double ratio(R_D) and direct photons(γ_{direct})

$$\gamma_{\text{direct}} = \gamma_{\text{incl}} - \gamma_{\text{decay}} \tag{1}$$

- Decay photons are simulated using MC techiques
- Inclusive photons are measured from the real data
- The raw cluster does not represent actual number of photons
- Need to evaluate the purity(P) of the sample
- Need to determine the efficiency(ϵ) of photon detection

$$E\frac{d^3N_{\gamma^{inc}}}{dp^3} = P \times \frac{1}{\epsilon} \times \left(\frac{1}{N_{\text{ev}}} \times \frac{1}{2\pi} \times \frac{1}{p_{\text{T}}} \frac{d^2N}{dp_{\text{T}}dy} \right) \tag{2}$$

Raw yield of clusters in PHOS for LHC18r (different centralities)

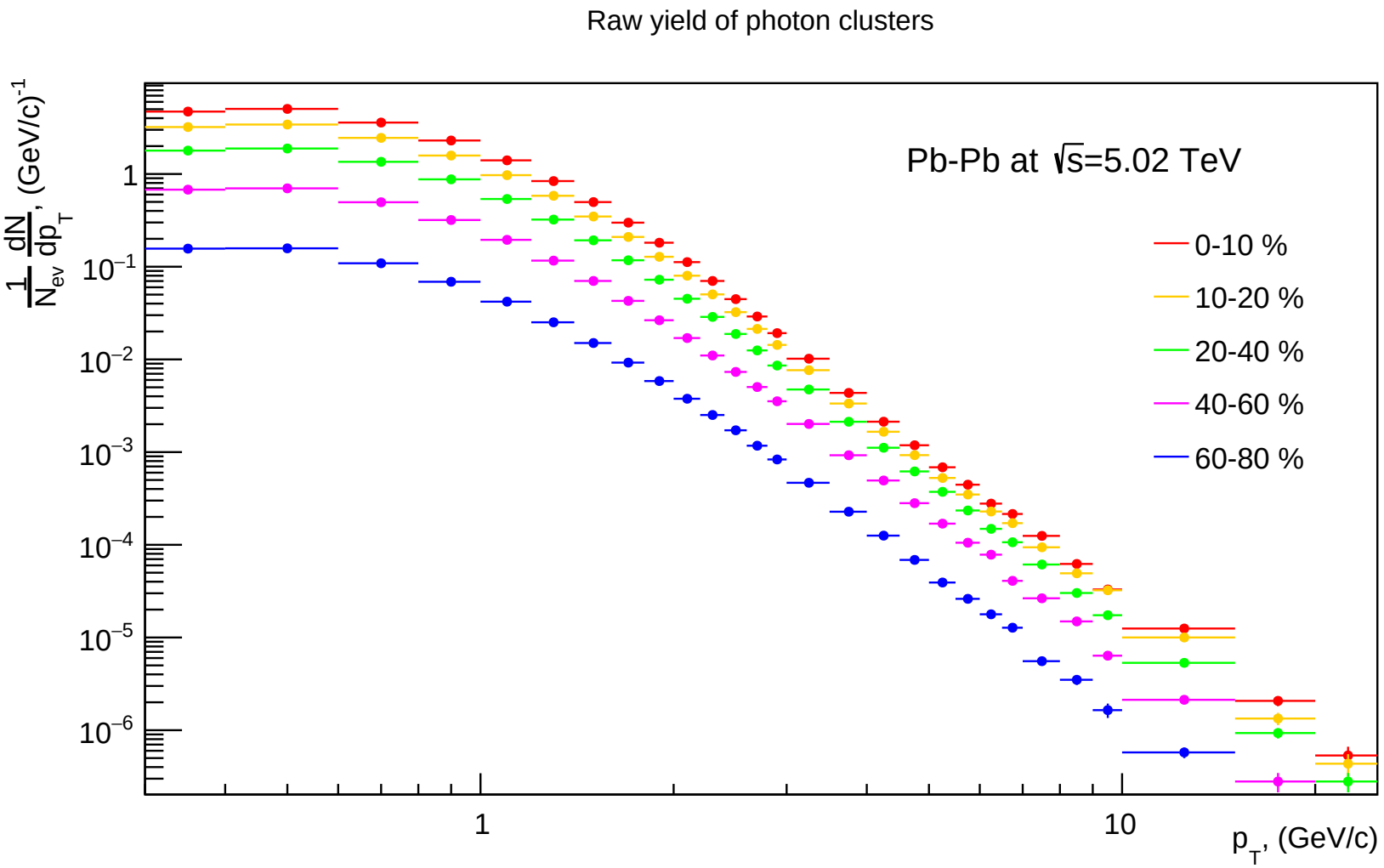

Contamination in the photon samples

$$N_{cluster} = N_{\gamma} + N_{e^{\pm}} + N_{\pi^{\pm}} + N_{K^{\pm}} + N_{p} + N_{\bar{p}} + N_{n} + N_{\bar{n}} + N_{K^{0}_{L}} + N_{K^{0}_{S}} + ...$$

- Not all clusters formed in PHOS are caused by actual photons. Many other particles deposit their energy and gets misidentified as photons thus contaminating the samples.
- Using MC data we can simulate the cluster formations from many possible sources
- The ionization loss in $PbWO_4$ for $\mu^{\pm}$ is very small compared to energy cut(< 0.3 GeV)
- Using charged particle veto detector(CPV) [and ITS detector] , the charged particles($e^{\pm}, \pi^{\pm}, K^{\pm}, p$) can be identified by extrapolating charged tracks. The clusters are removed if they are too close to the charged tracks
- Using dispersion filter(based on cluster characteristics, e.g. shower shape) we minimize contaminations of other particles including neutral particles(e.g. using isospin symmentry)
- K^0_S are identified through the off vertex photons from the casacde of decay, $K^0_S \rightarrow 2\pi^0 \rightarrow 4\gamma$ (feed-down-correction)

PHOS sample purity using vertex photons

$$Purity(p_T) = \frac{N_{\gamma_{clusters}}(p_T)}{N_{all_{clusters}}(p_T)}$$

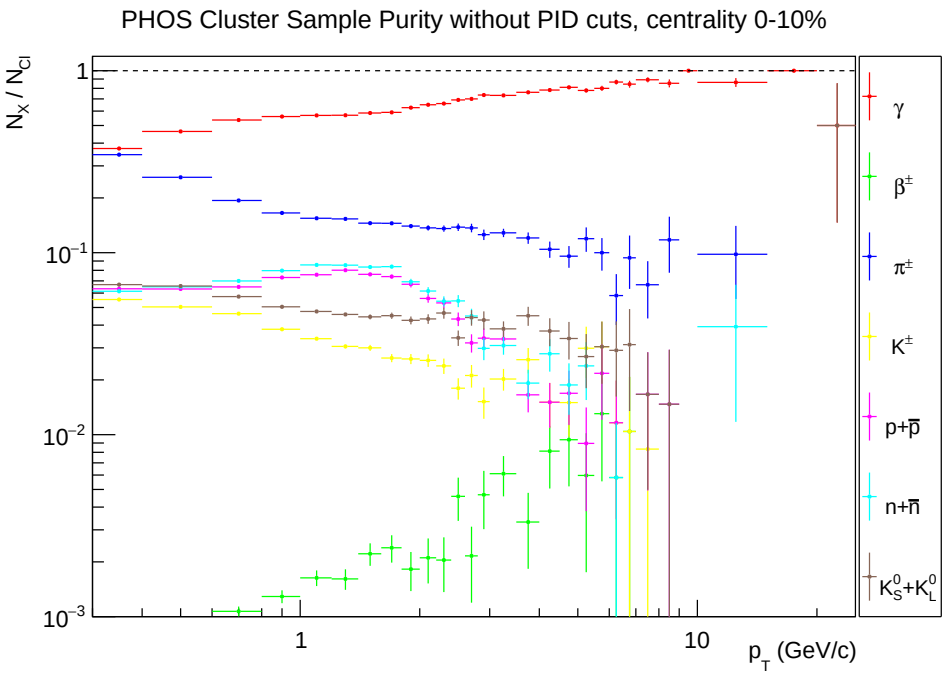

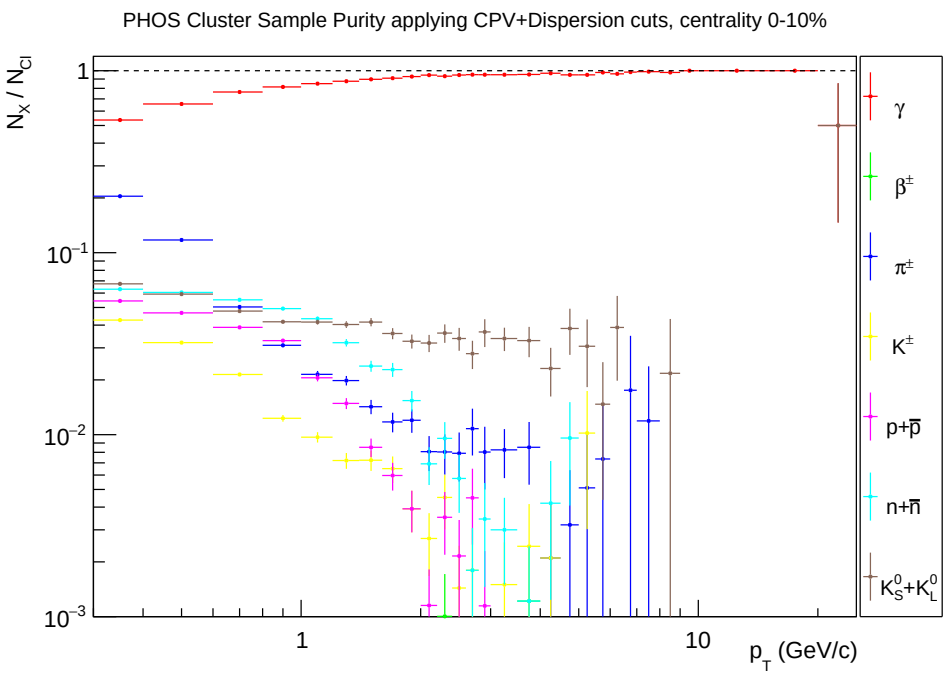

Efficiency of photon detection in PHOS

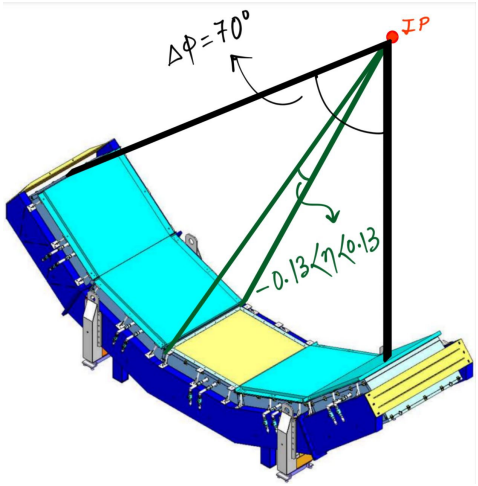

Figure: Modules of the PHOS detector and its angular coverage

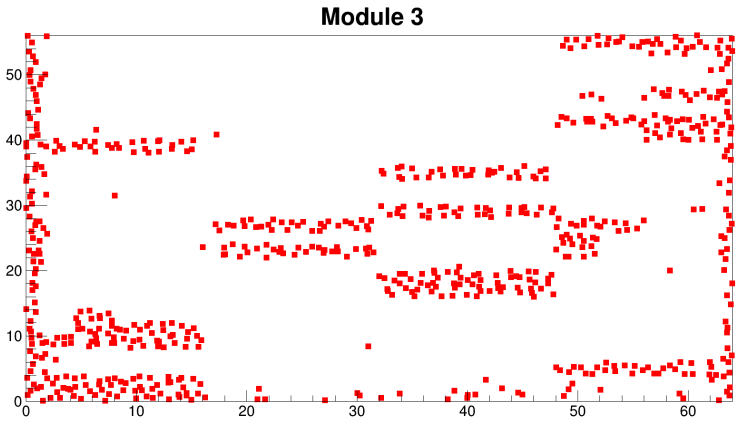

Figure: Red squares represent Bad channels, LHC18r Module3

- For photons emitted at mid-rapidity, $|y| < 0.5$, $0 < \phi < 2\pi$, only 5.1% of all photons fly into the PHOS solid angle.

- Photons can be caught inside an inactive channel
- Converted into electron-positron pair, which is deflected by magnetic field
- Entirely absorbed or dispersed by material of tracking detector
- Photons may impinge on calorimeter surface close to a charged particle
- Sometimes, photons may create shower similar to that of a hadron and be discarded

Efficiency for different centralities (applying CPV+Dispersion cut)

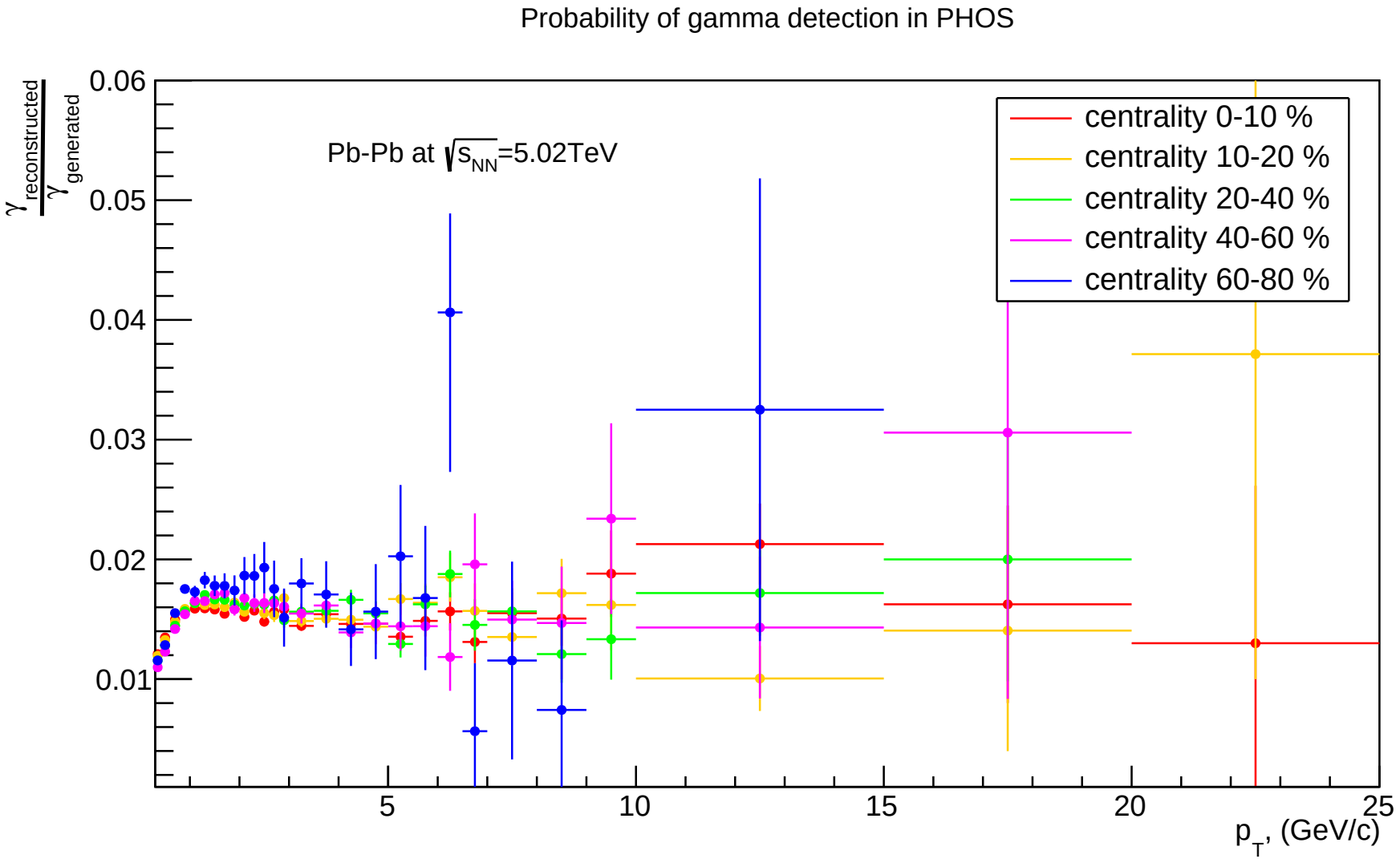

Invariant yield of inclusive photons : Different centralities

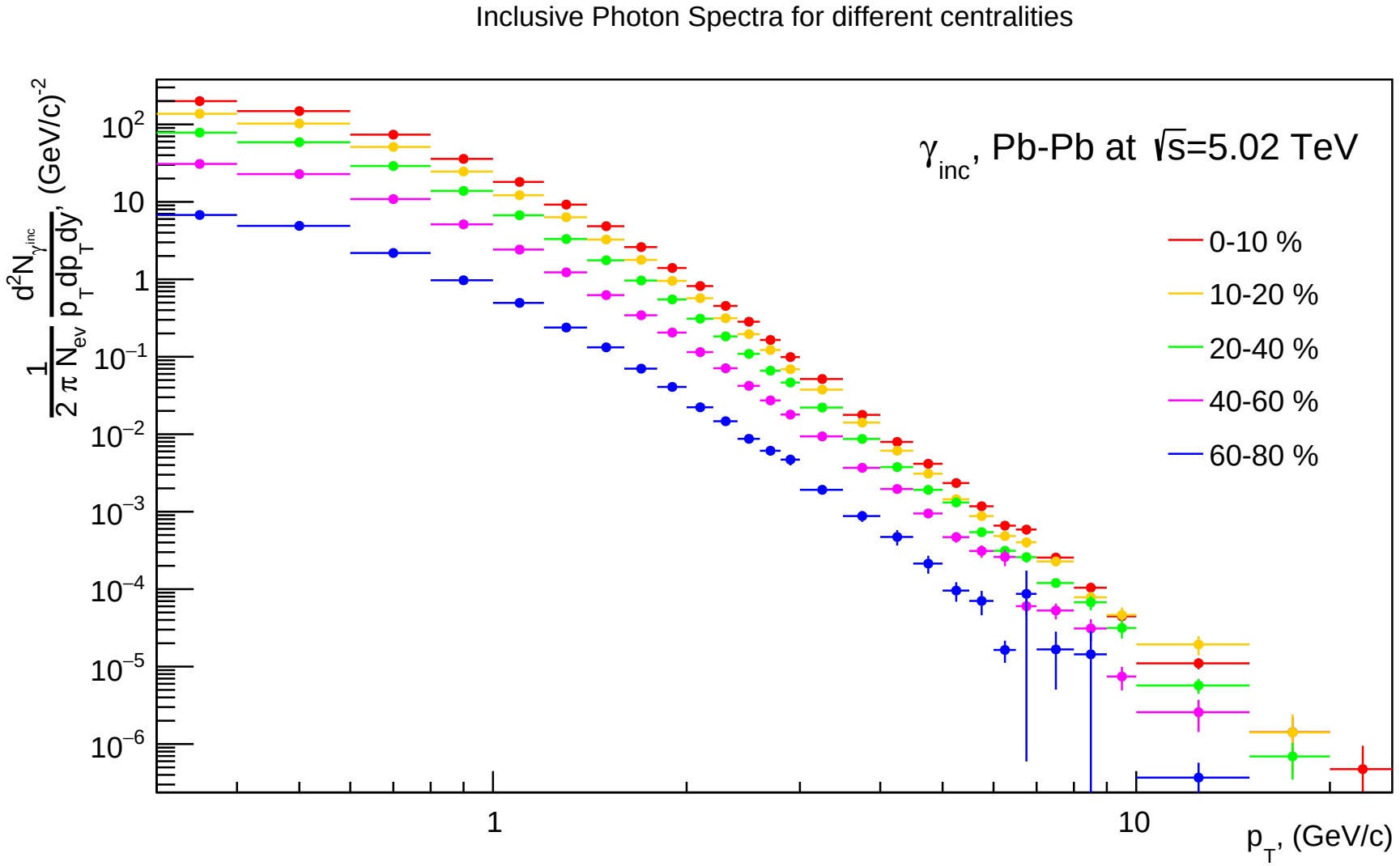

Background photon estimation using MC cocktail generation method

Particle	Mass (MeV/c^2)	Decay channel	Branching ratio (%)
π^0	135	$\gamma\gamma$	98.8
		$\gamma e^+ e^-$	1.2
η	547	$\gamma\gamma$	39.2
		$\gamma\pi^+\pi^-$	4.8
		$\gamma e^+ e^-$	4.9×10^{-3}
ω	782	$\pi^0\gamma$	8.3
		$\eta\gamma$	4.6×10^{-4}
η'	958	$\rho^0\gamma$	29.1
		$\omega\gamma$	2.8

Table: Particles decaying into photons

- **Hagedorn function** [5]: $\frac{d^2N}{dydp_T} = p_T \cdot A\left(\exp(ap_T + bp_T^2) + \frac{p_T}{p_0}\right)^{-n}$
  This functional form approaches an exponential at low p_T and a power law at larger transverse momenta and describes the measured spectra over full measured range
- **Transverse mass scaling :** $m_T = \sqrt{p_T^2 + m_0^2}$; $\frac{d^2N}{p_T dp_T dy} = \frac{d^2N}{m_T dm_T dy}$
  Transverse momenta spectra,
  $f_X(p_T, X) = C \times \frac{p_{T,X}}{\sqrt{m_{0,x}^2 + p_{T,x}^2 - m_{0,R}^2}} \times f_R(\sqrt{m_{0,x}^2 + p_{T,x}^2 - m_{0,R}^2})$

Hadronic decay from cocktail simulation

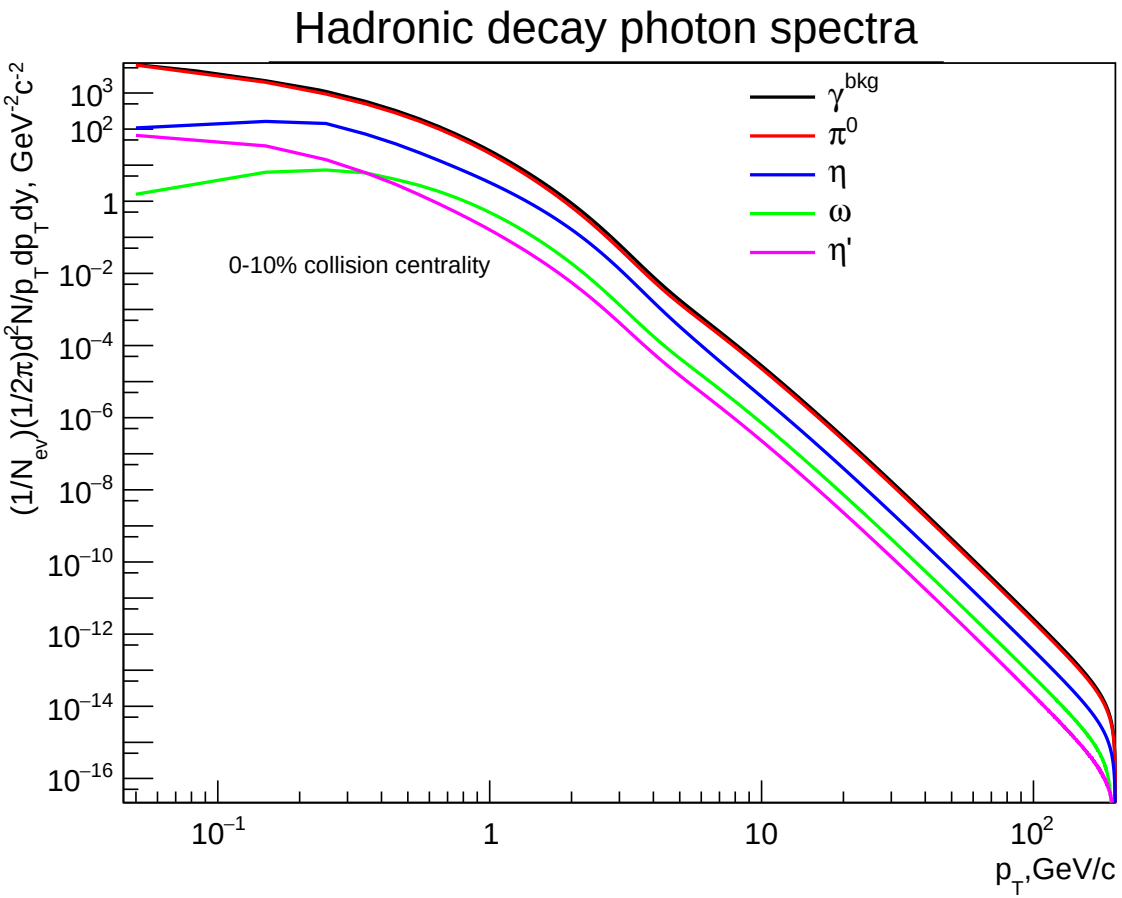

Figure: Shape of input hadrons and background photons

- π^0 and η mesons are generated using parametrization. ω and η' are generated using transverse mass scaling of π^0 spectra

Decay photon cocktail in Pb–Pb collisions at $\sqrt{s_{NN}} = 5.02$ TeV centrality 0-10 %

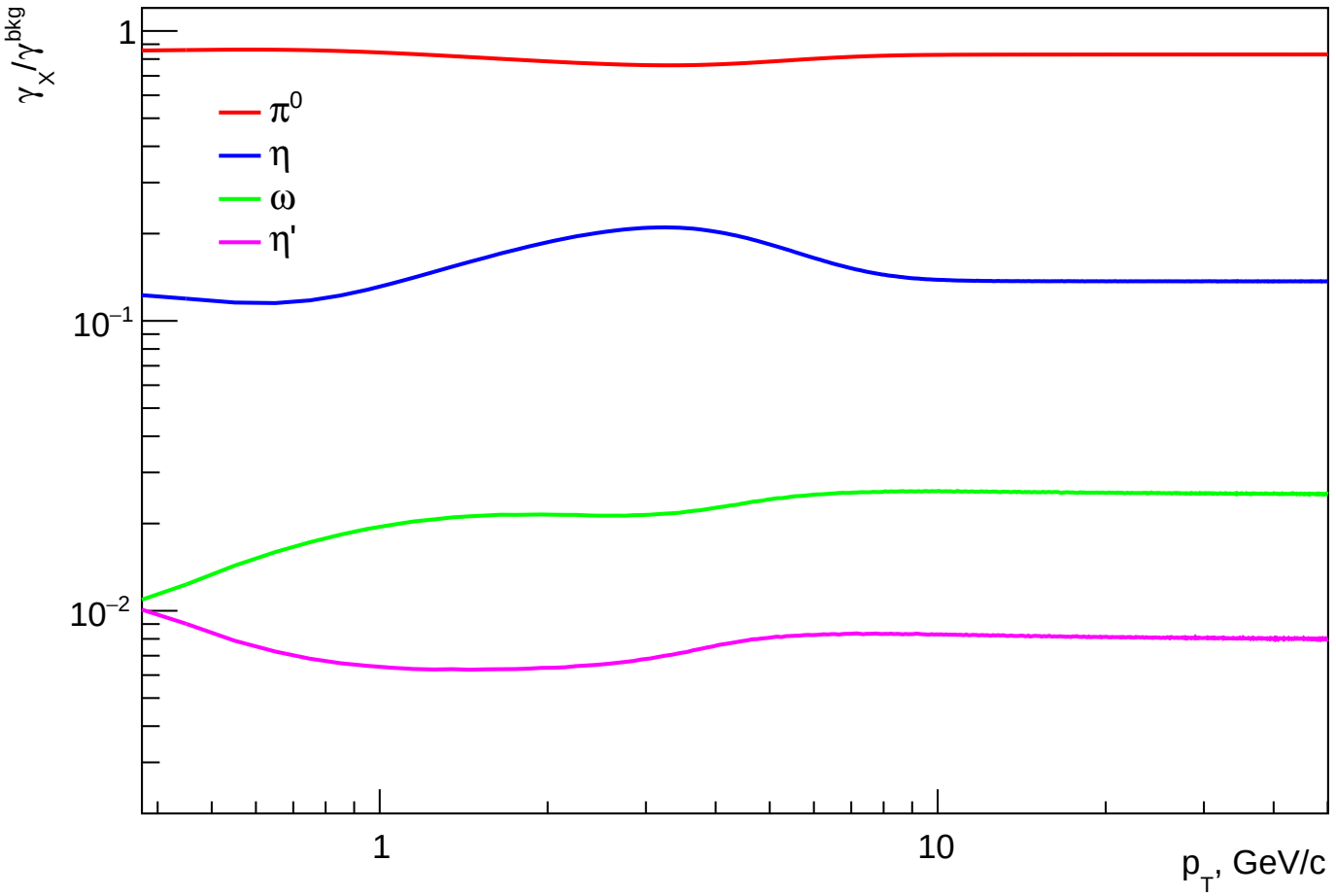

Figure: Fraction of various hadronic decay sources [π^0 ($\sim$ 90%) is the most dominant background]

Inclusive and decay photon spectra for centrality 0-10 %

compared with pertubative-QCD results (for different factorization scales)

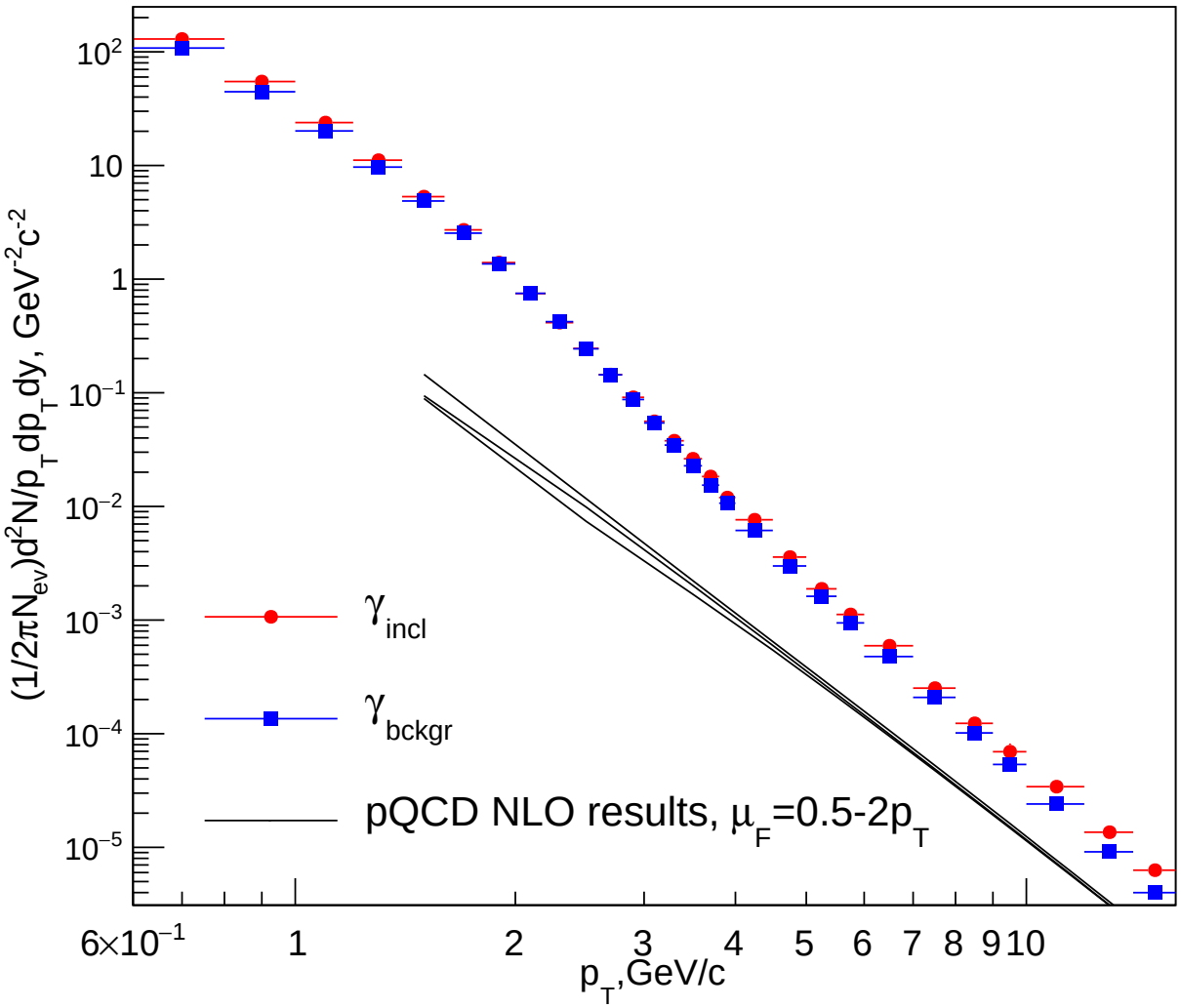

Double Ratio : To reduce systematic uncertainty

$$\text{Decay 1: } X \rightarrow A + B$$
$$\text{Decay 2: } X \rightarrow C + D$$

Problem: The detector has different efficiencies for detecting particles A, B, C, and D. This makes directly calculating the branching ratios inaccurate.

$T(X \rightarrow AB) =$ True number, $D(X \rightarrow AB) =$ Detected number, ε (A) etc.= Detection efficiencies

Single Ratio: The measured branching ratio of X decays would be:

$$\frac{D(X \rightarrow AB)}{D(X \rightarrow CD)} = \frac{\varepsilon(A) * \varepsilon(B) * T(X \rightarrow AB)}{\varepsilon(C) * \varepsilon(D) * T(X \rightarrow CD)}$$

Introducing a particle Y with similar decays and a known true branching ratio : R(Y) = $\frac{T(Y \rightarrow AB)}{T(Y \rightarrow CD)}$

Double Ratio:

$$\frac{D(X \rightarrow AB)/D(Y \rightarrow AB))}{D(X \rightarrow CD)/D(Y \rightarrow CD)}$$
$$= \frac{[\varepsilon(A)\varepsilon(B)T(X \rightarrow AB)]/[\varepsilon(A)\varepsilon(B)T(Y \rightarrow AB)]}{[\varepsilon(C)\varepsilon(D)T(X \rightarrow CD)]/[\varepsilon(C)\varepsilon(D)T(Y \rightarrow CD)]}$$

Direct photons(γ_{direct}) spectra using the Double ratio(R_D)

$$R_\gamma = \frac{\gamma^{\text{inc}}}{\gamma^{\text{decay}}} \approx \left(\frac{\gamma^{\text{inc}}}{\pi^0_{\text{meas}}}\right)_{\text{data}} \Big/ \left(\frac{\gamma^{\text{decay}}}{\pi^0_{\text{param}}}\right)_{\text{MC}} = R_D \tag{3}$$

$$\gamma_{\text{direct}} = \gamma_{\text{incl}} - \gamma_{\text{decay}} = \left(1 - \frac{1}{R_D}\right) \gamma_{\text{incl}} \tag{4}$$

Finally, the direct photons invariant yield can be calculated as follows,

$$\frac{1}{2\pi N_{\text{ev}}} \frac{d^2 N_{\gamma\, dir}}{p_{\text{T}} dp_{\text{T}} dy} = \frac{1}{2\pi N_{\text{ev}}} \frac{d^2 N_{\gamma\, inc}}{p_{\text{T}} dp_{\text{T}} dy} \left(1 - \frac{1}{R_D}\right) \tag{5}$$

Ongoing work: γ/π^0 ratios

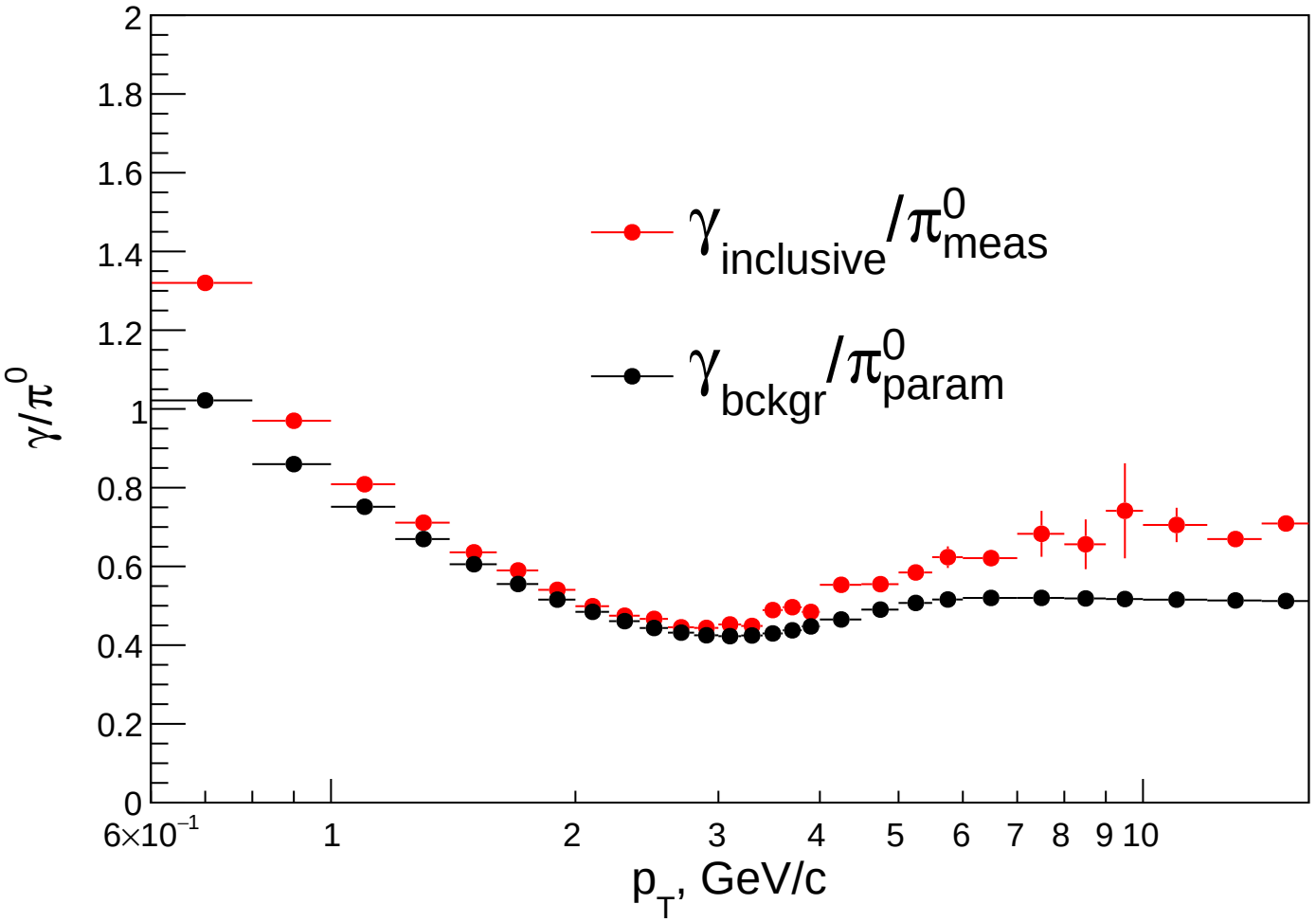

Ongoing work: π^0 ratios from data and MC for centrality 0-10 %

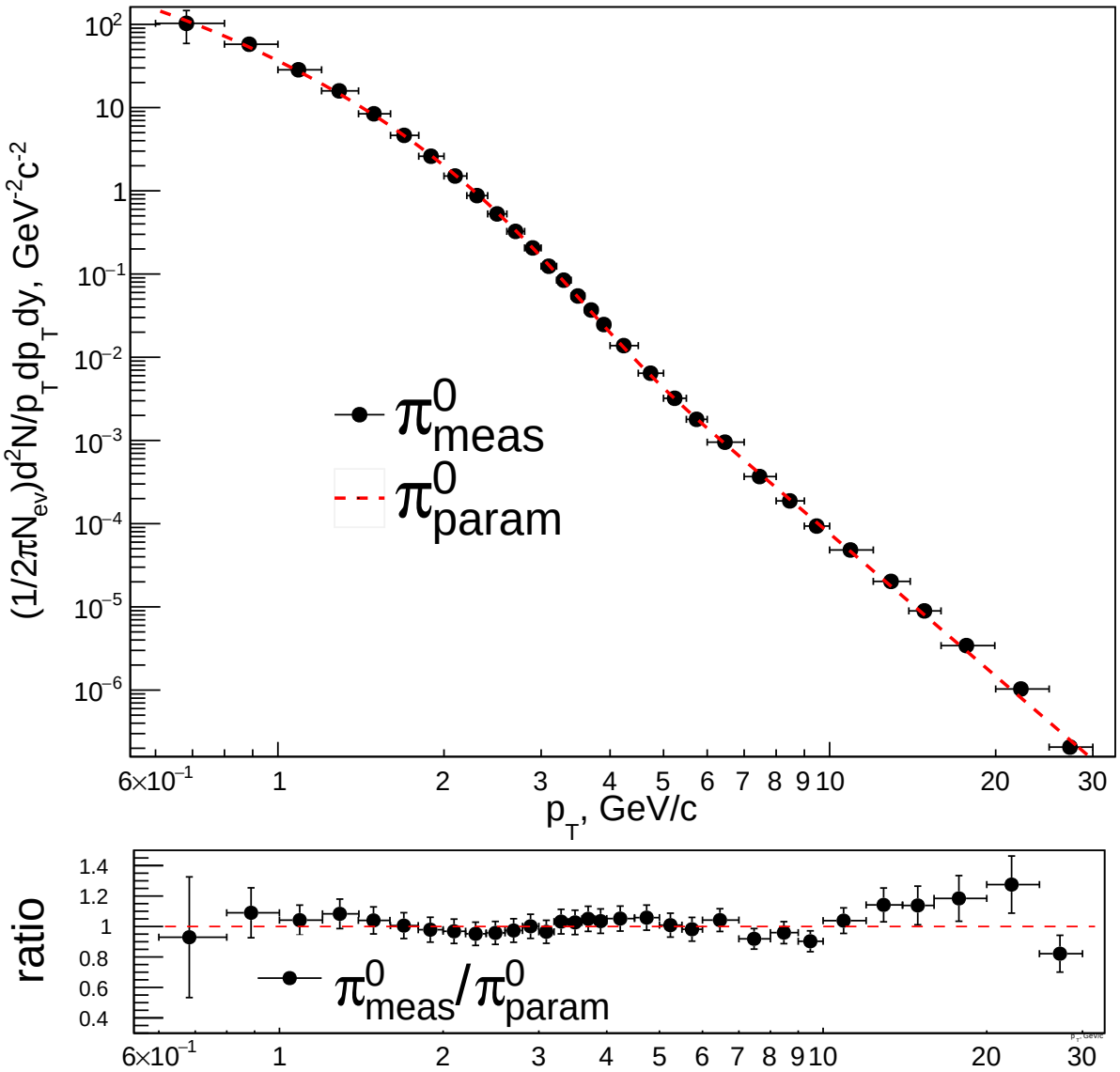

Ongoing work: Double ratio (0-10% centrality)

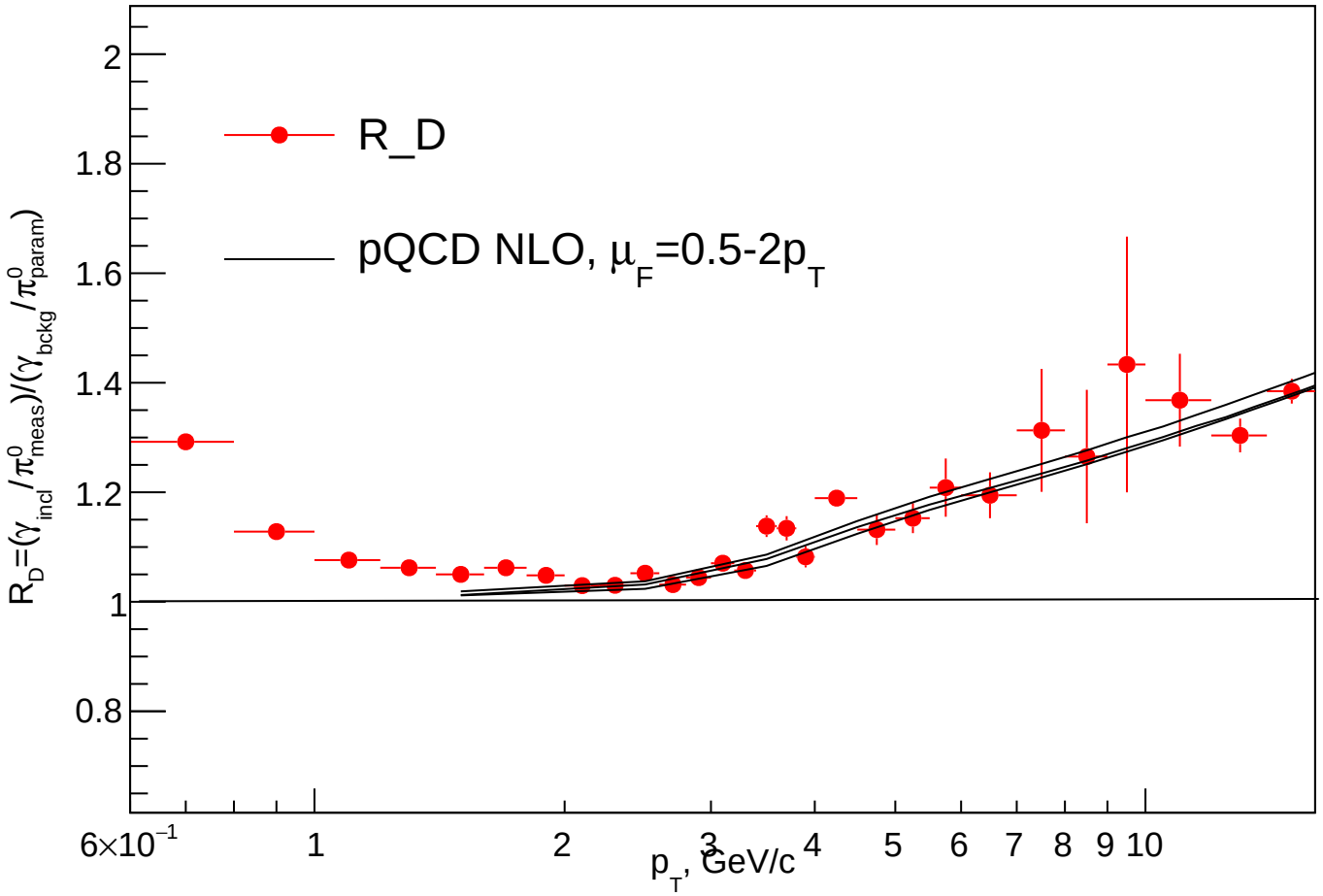

Previous results : Temperature estimation

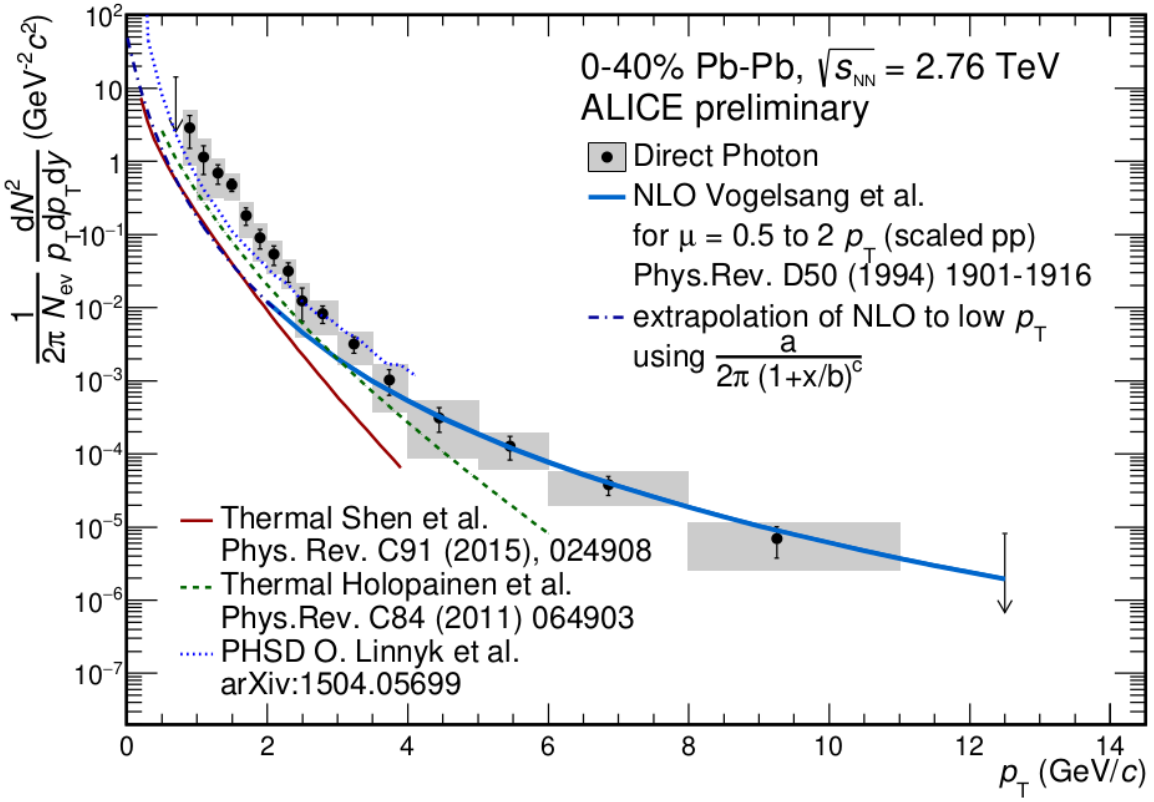

$$A \cdot \exp\left(-\frac{p_T}{T_{\text{eff}}}\right) \text{ for } p_T \leq 2.2\,\text{GeV/c}$$

$$T_{\text{eff}} = 304 \pm 51_{\text{stat+sys}}\,\text{MeV}\,(2.76\,TeV, \text{ALICE, LHC})$$

$$T_{\text{eff}} = 219 \pm 19_{\text{stat}} \pm 19_{\text{sys}}\,\text{MeV}\,(200\,Gev, \text{PHENIX, RHIC})$$

Elliptic flow : Previous results from PHENIX and ALICE

$$\frac{dN}{d\varphi} = \frac{N}{2\pi} \cdot (1 + \sum_{n>1} v_n cos(n[\varphi - \Psi_R]))$$

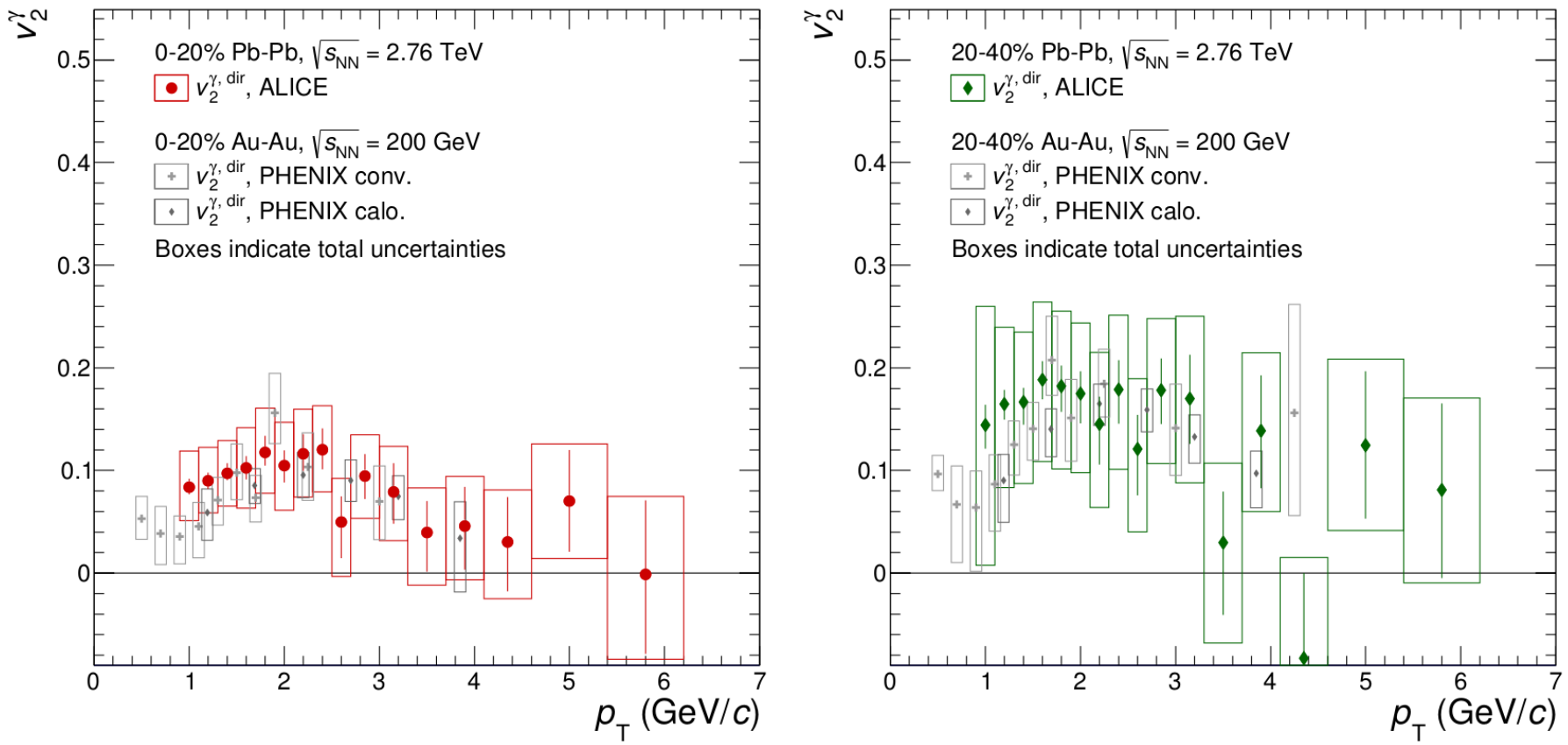

Figure: Elliptic flow of direct photons compared with PHENIX results for 0-20% (left) and 20-40% (right) centrality classes

[5] CERN-EP-2018-117

Summary

- In extreme conditions, the properties of QCD matters are not well understood
- Direct photon study of QGP is one way of contributing towards the understanding
- We have obtained the inclusive photon spectra and decay backgrounds
- We are working on the double ratio to obtain direct photon spectra

To obtain physically meaningful results(e.g. direct photon yield, size of thermal photons, elliptic flow etc.) on direct photon production which is a part of ALICE's effort to reach the following big goals

- To understand the formation of QGP and its properties
- Testing the predictions of Field QCD and Lattice QCD
- Understanding quark confinement and parton distribution functions within nucleons

THANK YOU FOR LISTENING!

BACKUP SLIDES

Ongoing work: Single ratio vs double ratio (0-10% centrality)

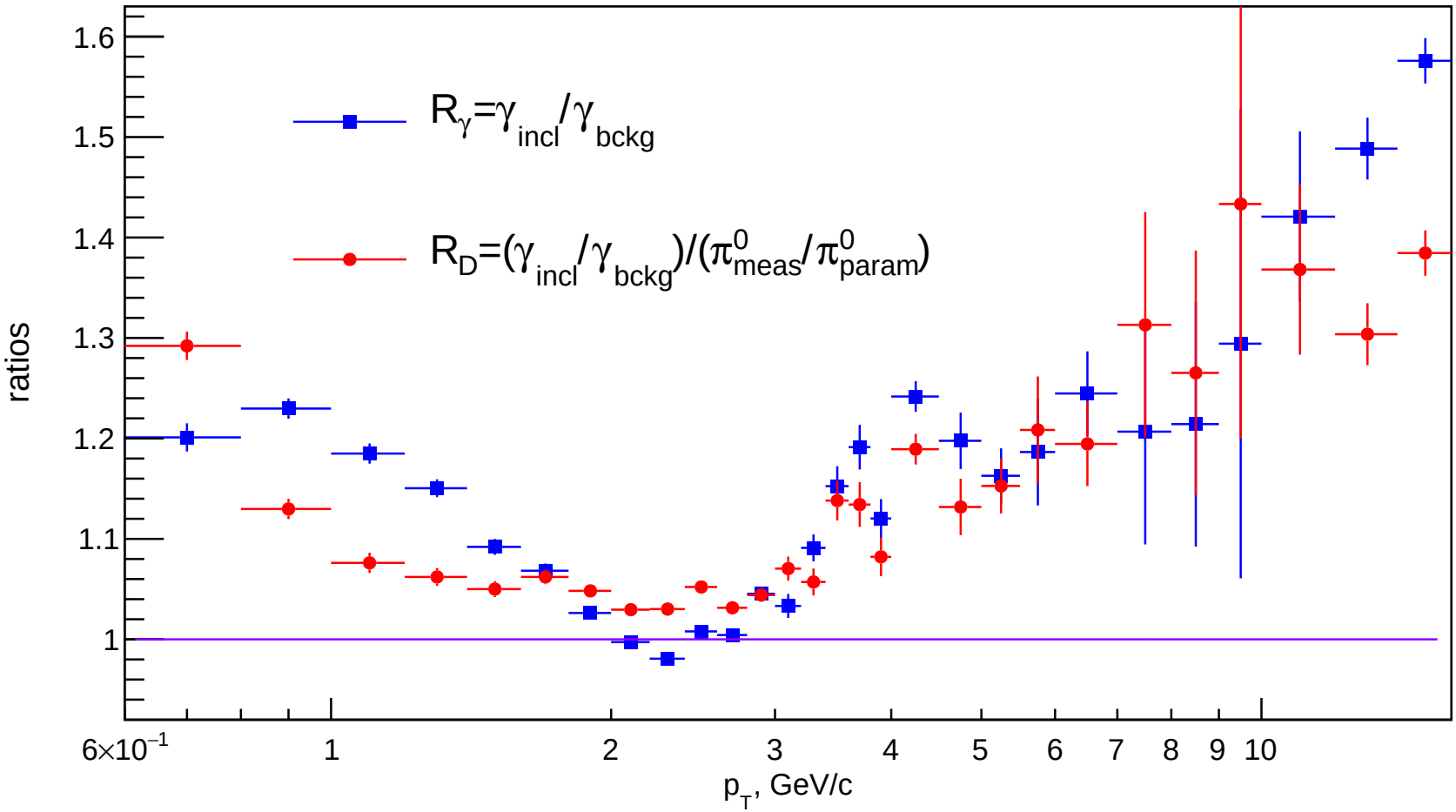

Previous results : Double ratio and direct photon spectra

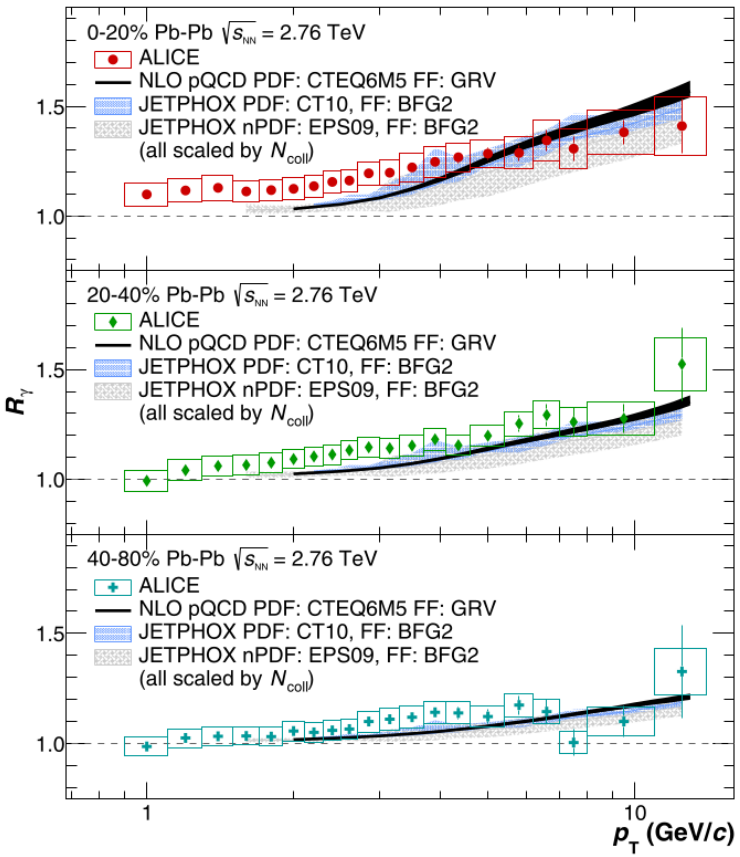

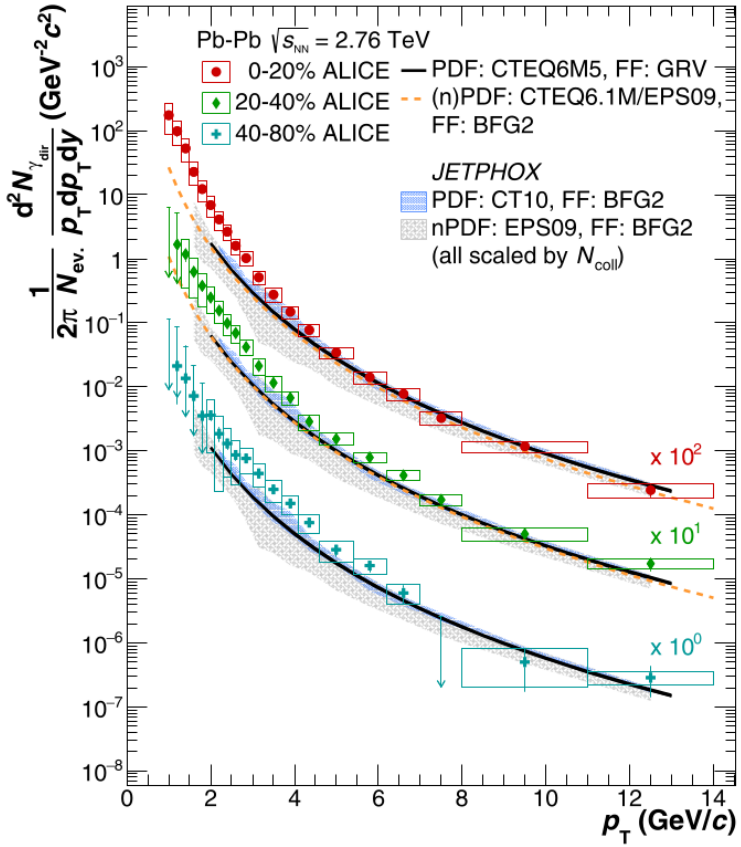

DDA, system of equations

$$
\begin{cases}
N_{cl} = & N_{\gamma} + N_{[\pi^{\pm}K^{\pm}]} + 2N_{[p\bar{p}]} + N_X, \\
N_{cl}^{CPV} = & C_{\gamma}^{CPV} N_{\gamma} + C_{\pi^{\pm}}^{CPV} N_{[\pi^{\pm}K^{\pm}]} + (C_{\pi^{\pm}}^{CPV} + C_{\gamma}^{CPV}) N_{[p\bar{p}]} + C_X^{CPV} N_X, \\
N_{cl}^{Disp} = & C_{\gamma}^{Disp} N_{\gamma} + C_{\pi^{\pm}}^{Disp} N_{[\pi^{\pm}K^{\pm}]} + 2C_{p\bar{p}}^{Disp} N_{[p\bar{p}]} + C_X^{Disp} N_X, \\
N_{cl}^{CPV+Disp} = & C_{\gamma}^{CPV} C_{\gamma}^{Disp} N_{\gamma} + C_{\pi^{\pm}}^{CPV} C_{\pi^{\pm}}^{Disp} N_{[\pi^{\pm}K^{\pm}]} + \\
& (C_{\pi^{\pm}}^{CPV} + C_{\gamma}^{CPV}) C_{p\bar{p}}^{Disp} N_{[p\bar{p}]} + C_X^{CPV} C_X^{Disp} N_X,
\end{cases}
$$